Green Chemistry

PAPER

View Article Online
View Journal | View Issue

Check for updates

Cite this: *Green Chem.*, 2024, **26**, 5477

Production of lignin containing cellulose nanofibrils (CNF) after enzymatic treatment of curl-induced, unbleached kraft pulps†

Jie Wu, [a] Yintian Dong,[a] Xia Sun, [b] Peipei Wang,[c] Jiaying Zhu,[b] Yeling Zhu, [b] Feng Jiang [b] and Jack Saddler *[a]

Received 18th February 2024,
Accepted 28th March 2024

DOI: 10.1039/d4gc00834k

rsc.li/greenchem

Lignin-containing cellulose nanofibrils are successfully produced after enzymatic treatment of curl-induced, unbleached kraft pulps. An enzyme cocktail composed predominantly of endoglucases but also containing xylanases, laccases, and lytic polysaccharide monooxygenases (LPMO's) results in significant enzyme-mediated fiber modification. A substantial (70%) reduction in pulp viscosity can be achieved while enzyme treatment of curl-induced fibers results in improved fibrillation and increased colloidal stability. This is likely due to the higher negative charge density (−57.5 mV) of the fibers. The enzyme-treated, curl-derived cellulose nanofibrils show improved characteristics such as higher transmittance, lower viscosity, and thinner nanofibrils, resulting in enhanced nano-fibrillation. Superior mechanical properties, such as increasing the tensile strength of cellulose nanopapers to 150 MPa, are obtained as a result of the improved fibril network. The pre-curled fibers appear more accessible to enzyme treatment, resulting in cellulose nanofibrils with improved properties with less chemical treatments and mechanical refining energy required.

Published on 02 April 2024. Downloaded on 5/26/2026 6:16:00 AM.

1. Introduction

Cellulose is arranged in fibrils at the nano, micro and macro scale in nature, using inter and intra molecular hydrogen bonding, while it is also closely intertwined with hemicellulose and lignin.[1–3] Past work has shown that swelling and fibrillation of the cellulose fibril enhances the overall cellulose surface area, typically also enhancing fiber characteristics such as strength, rheology and thermal stability, leading to advanced functional applications such as cellulose membranes, elastic aerogels and supercapacitors.[4–9] However, fibrillation is usually achieved by mechanical and/or chemical treatments while any association with lignin can significantly hinder fibrillation.[10]

Earlier work has shown that the supramolecular structure of wood derived cellulose is not evenly distributed, with certain areas within the fibers, known as micro-compressions, slip planes, dislocations and kinks, less ordered in their structure.[11–13] These less organized regions are thought to result from the inherent twist of cellulose fibrils, resulting in a weakening of the hydrogen bonds within the more ordered regions within the fiber.[11–13] These less organized regions within the fibers can also be introduced by longitudinal compression of the cell wall during pulping,[14] have a lower crystallinity[15] compared to the bulk cell wall, and have a weaker tensile behavior at the nano scale.[12,14] Related work has also shown that this increase in cellulose accessibility enhances enzyme-mediated deconstruction of cellulose, even at high solids loadings.[11]

Although cellulase enzymes have been predominantly assessed for their ability to deconstruct cellulose, related work has shown that they can be used to result in beneficial pulp modifications.[16] In particular, endoglucanase have been used to facilitate pulp fibrillation[17,18] while reducing the energy required for subsequent mechanical fibrillation.[19] Additional beneficial effects can be obtained when endoglucanases are synergized with other accessory enzymes such as xylanases and lytic polysaccharide monooxygenases (LPMO's).[17,20] Other work has shown that LPMOs, which can oxidize cellulose, can offer a greener alternative to chemical modifications with chemicals such as TEMPO.[21–23]

As enzyme accessibility has been shown to be a major impediment to effective cellulose modification, recent work

[a]*Forest Product Biotechnology/Bioenergy Group, Department of Wood Science, University of British Columbia, 2424 Main Mal, Vancouver, V6T 1Z4, Canada. E-mail: jack.saddler@ubc.ca*
[b]*Sustainable Functional Biomaterials Lab, Department of Wood Science, University of British Columbia, 2424 Main Mall, Vancouver, British Columbia, V6T 1Z4, Canada*
[c]*Bioproducts Institute, Department of Chemical and Biological Engineering, Department of Chemistry and Department of Wood Science, University of British Columbia, 2385 East Mall, Vancouver, BC, V6T 1Z3, Canada*

† Electronic supplementary information (ESI) available. See DOI: https://doi.org/10.1039/d4gc00834k

Published on 02 April 2024. Downloaded on 5/26/2026 6:16:00 AM.

has suggested that introducing less-organized regions in the pulp fibers, through the induction of curl,[11] might enhance the selective action of an enzyme cocktail when trying to hydrolyze the cellulose component. Although the occurrence of lignin has been shown to hinder the fibrillation of cellulose fibers,[24] removing most of the lignin *via* processes such as bleached kraft pulp, is economically challenging. Alternatively, unbleached kraft pulp (also known as brown stock) might be a more sustainable alternative as it is cheaper feedstock, has a lower lignin content than thermomechanical pulp (TMP) and might be more receptive to selective enzyme treatment when trying to produce cellulose nanofibrils (CNF). Recent work has shown that lignin-containing cellulose nanofibrils have beneficial properties such as enhanced UV absorption and increased hydrophobicity, increasing their compatibility with other hydrophobic polymers.[17,25,26]

One goal of this work was to assess the possibility of enhancing enzyme-mediated pulp modification by building on mechanically induced fiber curling. This latter process has been shown to generate less organized regions that are more accessible to enzymes, possibly making fibers more prone to fibrillation during mechanical treatments. In the work reported below, more accessible, less organized fiber regions were introduced into an unbleached kraft pulp (brown stock) by prior fibrillation. This was followed by enzyme treatment, using different enzyme cocktails and further refining, to successfully produce highly fibrillated, lignin containing CNF, which was more hydrophobic than conventional CNF.

2. Experimental section

2.1 Chemicals and substrate

Sodium acetate, acetic acid and copper(II) ethylenediamine solution were purchased from Fisher Scientific. The unbleached Softwood kraft pulp (brown stock) was composed of 77% cellulose, 9% xylan, 8% mannan, 0.7% arabinan, 0.4% galactan and 6% lignin.

2.2 Curl and enzyme treatment

Curl treatment of unbleached Softwood kraft pulp was performed using a KitchenAid mixer equipped with a conventional mixing head (Kitchenaid professional 6000hd mixer) at high solid loading of 20 wt% on speed setting "5" for 1 hour, following the methods described by Chandra *et al.*[11]

The enzymes were generously provided by Novozymes (Denmark). Enzyme treatments of unbleached kraft pulp were conducted in a shaking incubator at 50 °C, 180 rpm. Prior to enzyme addition, the pulp was mixed with a sodium acetate buffer (pH 4.8) to obtain a 2 wt% solids loading.

Enzyme treatments to achieve cellulose hydrolysis were performed at a 2 wt% solids and a protein loading of 20 mg CTec per 3 g cellulose for 24 hours. Samples were collected at 1, 2, 3, 4, 5, 6, and 24 hours. The glucose released (in the supernatant after centrifugation) was determined using a YSI glucose analyzer. The hydrolysis yield was determined by the method described in the reference Wu *et al.*[27] A fiber quality analyzer (FQA) was used to assess fiber morphology by measuring greater than 5000 fibers suspended in deionized water. This measurement reported values including mean fiber length, aspect ratio (calculated as the ratio between fiber length and width), and curl index (calculated as $(L/\ell) - 1$, where L and ℓ stand for fiber contour length and end-to-end length, respectively).

Enzyme mediated fiber modification was conducted at 2 wt% solids and a protein loading of 10 mg g^{-1} cellulose for 6 hours. The enzyme cocktail included endoglucanases, xylanases, LPMOs, and laccases at a ratio of 4 : 2 : 2 : 2. After enzyme treatment, the pulp was extensively washed with distilled water, filtered and stored at 4 °C for further processing.

The viscosity of pulps before and after enzyme treatment was determined using TAPPI T 230 method as an indicator of cellulose DP.

2.3 Morphology of enzyme-treated pulp

The morphology of enzyme-treated pulp after micro-fibrillation was observed under the polarization mode using a Nikon Eclipse LV100POL optical microscope equipped with a $\frac{1}{4}\lambda$ plate, camera and using NIS microscope imaging software. The samples were also air-dried on conductive tape and observed with Helios NanoLab 650 FIB-SEM.

2.4 Water retention value

The water retention values (WRV) of pulps were conducted in duplicate, according to the method described by Wu *et al.*[28] In brief, 0.5 g (dry weight) of pulp was soaked in deionized water overnight, after being diluted and drained out, the wet pad was centrifuged at 3000*g* for 15 minutes.

2.5 Micro and nano fibrillation of enzyme-treated pulps

Micro-fibrillation of enzyme treated unbleached kraft pulp was carried out in a kitchen blender (Vitamix E310) at 1 wt% solids loading (0.2 g in 200 mL distilled water) for 30 minutes. Nano-fibrillation of micro-fibrillated pulp was carried out in a microfluidizer (Nano DeBEE) at 0.5 wt% consistency for 10 passes, using the Z05 nozzle that has a size of 0.13 mm, following protocol reported by Jiang *et al.*[29]

2.6 Characterization of CNF suspensions

The zeta-potential of (0.1 wt%) CNF suspensions was measured using a Zetasizer nano-ZS DLS (Malvern). The transmittance of (0.05 wt%) CNF suspensions was measured in a quartz cuvette by a UV-vis spectrometer (Cary 50 UV-Vis, Agilent). The viscosity of (0.5 wt%) the CNF suspensions was tested using AR-G2 controlled stress rheometer by TA Instrument, which is equipped with 60 mm parallel plate. The shear rate range was 0.01 to 1 s^{-1}, with total of 30 data points logarithmically equidistant to one another. The morphology of CNF was observed through transmission electron microscope (TEM, Tecnai Spirit), where 0.01 wt% of CNF suspension on a glow-discharged formvar-carbon copper grid was negatively stained with 2% uranyl acetate and then observed under 120

 This journal is © The Royal Society of Chemistry 2024

Published on 02 April 2024. Downloaded on 5/26/2026 6:16:00 AM.

kV accelerating voltage. The width of CNF was measured by ImageJ software.

2.7 Preparation cellulose nanofibrils-derived cellulose nanopapers

A suspension containing 50 mg of dry weight of nano fibrillated cellulose was diluted with 45 mL of a solvent. The mixture was homogenized using a Fisher Homogenizer 850 for 30 seconds to ensure uniform dispersion of the cellulose fibrils. The homogenized mixture was then filtered under vacuum through a 0.45 μm PES membrane. The resulting filtered cellulose nanopaper was placed between two pieces of filter paper (Fisher Filter paper P8) and pressed for 4 hours to remove excess water. Afterward, the cellulose nanopaper was completely dried at room temperature for a minimum of 12 hours.

2.8 Mechanical strength, hydrophobicity, and UV-blocking effect of cellulose nanopapers

The tensile properties of different cellulose nanopapers were tested on a Uniaxial Materials Testing System (Instron 5969) with a load cell of 500 N and a crosshead speed of 2 mm min^{-1}. The prepared nanopapers were made into rectangular shapes with a length of 10 mm, a width of 4 mm, and a thickness of *ca.* 0.04 mm prior to the measurement.

Hydrophobicity of cellulose nanopapers was determined by water contact angle measurement using a tensiometer (Biolin, Theta Flex 300, Sweden) with a *ca.* 5 μm drop of distilled water on the surface of the nanopaper.

The UV-blocking effect of cellulose nanopapers was also measured by the UV-vis spectrometer (Cary 50 UV-Vis, Bruker), where the transmittance of lights from wavelength of 200 nm to 400 nm to the quartz cuvette with and without the presence of cellulose nanopapers was recorded.

3. Results and discussion

3.1 Impact of curl-treatment on effectiveness of enzyme-mediated hydrolysis of cellulose

As previous work had indicated that the introduction of less-organized fiber zones within pulp substrates enhanced enzyme accessibility and overall cellulose hydrolysis fibers,[11] we first wanted to assess if an unbleached kraft pulp that had been subjected to curl treatment (referred to as "curl fibers") was more susceptible to hydrolysis than a treated pulp (referred to as "straight fibers") when using the CTec3 cellulase cocktail (Fig. 1). It was apparent that the curl-induced pulps were much more easily hydrolyzed (Fig. 1a) and that, after 24 hours, more fines (particles size, 0.07–0.2 mm) were generated (Fig. 1b).

However, as the goal of the work was to minimize cellulose deconstruction and maximize beneficial pulp modification, an enzyme cocktail that lacked cellobiohydrolyases (CBHs), which have been shown to be primarily responsible for the hydrolysis of glucan chains,[30] but contained endoglucanases and the accessory enzymes, xylanases, lytic polysaccharide monooxygenases (LPMOs) and laccases, was used at lower enzyme loadings. It was hoped that the various accessory enzymes would facilitate access of the endoglucanases to the cellulose. Recent work had shown that xylanases could remove residual xylan, increasing accessibility to the cellulose.[31] In related work, LPMO's had been shown to cleave glycosidic chains by oxidizing the C_1 or C_4 carbon on the glucose unit,[32,33] with the oxidized cellulose carrying a negative charge when resuspended in water. Other work had also shown that the action of LPMO's also influenced cellulose structure, by increasing fibrillation, likely releasing tension stress and enhancing cellulase accessibility.[23] As laccases have been shown to increase the amount of phenolic compounds available from lignin containing substrates, resulting in an increase in LPMO activity by providing electron donors or reductive cofactors for LPMO activation,[34]

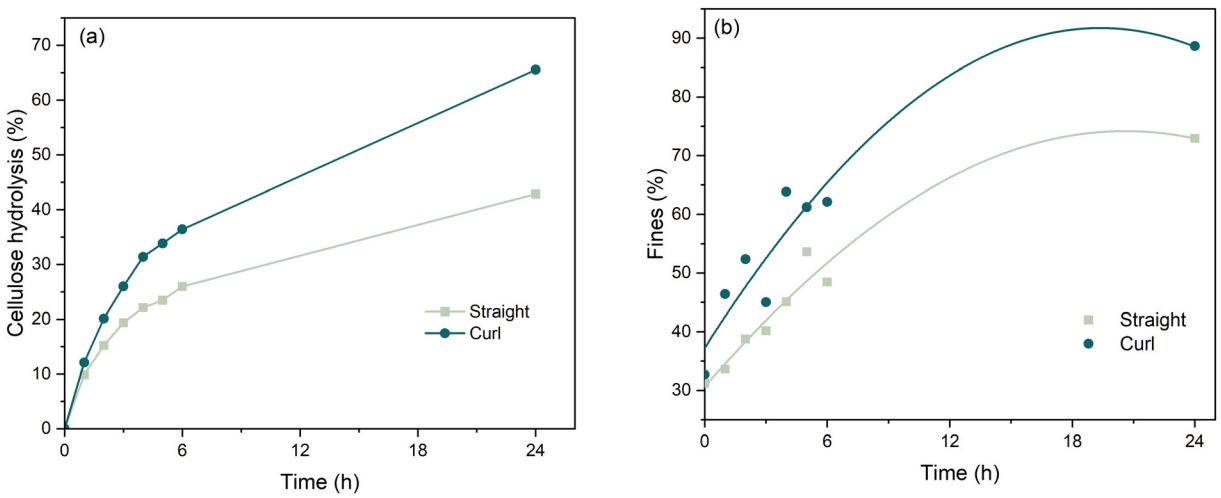

Fig. 1 Cellulose hydrolysis yield (a) and the percentage of fines generated during the enzymatic hydrolysis (b) of straight and curl fibers using the commercial cellulase enzyme cocktail (CTec 3).

Published on 02 April 2024. Downloaded on 5/26/2026 6:16:00 AM.

Table 1 Fiber morphology of pulp before and after enzyme treatment (mixture lacking CBH activity) and micro-fibrillation (blender) treatment

	Mean fiber length (mm)		Aspect ratio		Fines content (%)		Mean curl index	
Sample	Straight	Curl	Straight	Curl	Straight	Curl	Straight	Curl
Starting pulp	1.33	1.12	48.8	40.5	31.2	32.7	0.11	0.34
Enzyme treated	0.79	0.99	26.6	39.7	32.5	29.5	0.12	0.28
Enzyme and blender treated	0.18	0.23	5.4	7.5	67.6	59.2	0.12	0.07
Blender treated	0.9	—	32.9		41.9	—	0.05	—

these enzymes were also added to the cocktail. It is likely that the combined action of endoglucanases and accessory enzymes facilitates fibrillation after subsequent mechanical treatments.

When this enzyme cocktail was added to an unbleached kraft pulp for 6 hours, fiber quality analysis (FQA) indicated that there was a small reduction in fiber length (Table 1) which was likely due to endoglucanase action slightly reducing the degree of polymerization (DP) of cellulose,[35] although there was minimum yield loss due to the lack of CBHs. Scanning electron microscopy (SEM) also indicated that the "kinked" regions seemed to be more disrupted compared to the surface of straight fibers (Fig. S1†). When pulp viscosity was assessed using cupriethylenediamine (CED) dissolution (which is directly associated with the DP of the cellulose),[36] a significant reduction (70%) in the viscosity of the enzyme treated refined/curled fibers was observed (Fig. 2). However, enzyme treatment of both pulps did not result in significant changes to the crystallinity index of either pulp (Fig. S2†), indicating that the enzyme treatment had not resulted in any major changes to the crystalline structure of the cellulose.

3.2 Micro and nano-fibrillation of enzyme-treated fibers

As previous work had shown that low-consistency pulp refining could be simulated by using a kitchen blender,[37] it was used to reduce the particle size of straight and curl fibers so that they could pass through the microfluidizer nozzles during the subsequent nano-fibrillation. It was apparent that the cocktail containing endoglucanases and accessory enzymes resulted in a significant reduction in fiber length of curl and straight fibers after micro-fibrillation, while the original pulp fibers were more resistant to mechanical disintegration, as indicated by the retention of fiber length (Table 1). As well as reducing the particle size of the pulp, it was hoped that prior, low-consistency pulp refining would also increase the surface area of the fibers pulp by both external fibrillation and internal delamination. The water retention value (WRV), which is a well-established method for measuring a pulp's ability to hold water,[38] indicated that the enzyme cocktail treatment did not result in any distinguishable differences between refined and unrefined pulps. However, subsequent mechanical treatment resulted in a significant impact, as the curl treatment improved the WRV (50%) of the pulp following the combined treatment of endoglucanases/accessory enzymes and micro-fibrillation (Fig. 3a). Using polarized light microscopy, an increase in the presence of fibrils on micro-fibrillated curl fibers was apparent, while samples derived from straight fibers were mostly fragmented (Fig. 3c). This suggested that curl treatment induced increased disorganization within the fibers after enzyme treatments, resulting in a higher degree of fibrillation rather than undesired fiber cutting during mechanical treatment.

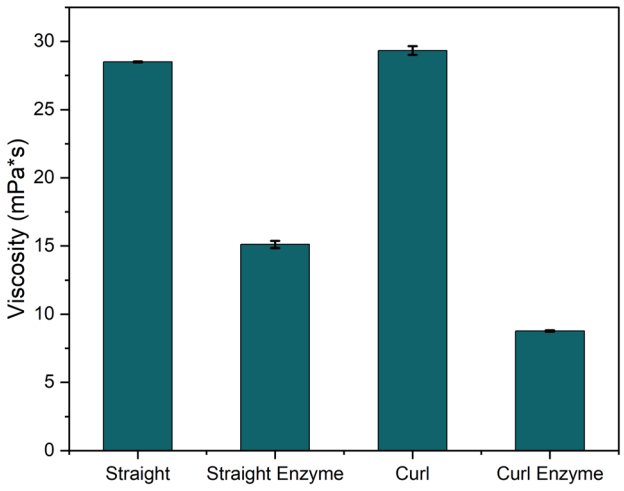

Fig. 2 Viscosity of cupriethylenediamine (CED)-dissolved kraft pulps. The pulps consist of straight and curl fibers before and after treatment with an enzyme mixture lacking CBH activity.

As mentioned earlier, the presence of negative charges on micro/nano-fibrillated cellulose contributes to increased colloid stability. Micro-fibrillated cellulose derived from curl fibers exhibited greater stability, likely due to the enhanced action of LPMO, which induces negative charges on the cellulose surface (Fig. 3b). This was confirmed by zeta potential measurement when the micro-fibrillated cellulose was subsequently processed by a microfluidizer to induce nano-fibrillation. It has been widely recognized that the absolute value of zeta potential greater than 30 mV is required for stable nanocellulose dispersion in water.[39] Both substrates achieved this requirement, with nanocellulose derived from curl fibers being even more negatively charged (−57.5 mV) than that of straight fibers (−40.3 mV) (Fig. 4a).

The greater charge density of curl-derived CNF indicated enhanced action of LPMOs on curl fibers, which could also lead to enhanced accessibility of cellulose to other enzymes such as endoglucanase, resulting in greater degree of nano-

 This journal is © The Royal Society of Chemistry 2024

Published on 02 April 2024. Downloaded on 5/26/2026 6:16:00 AM.

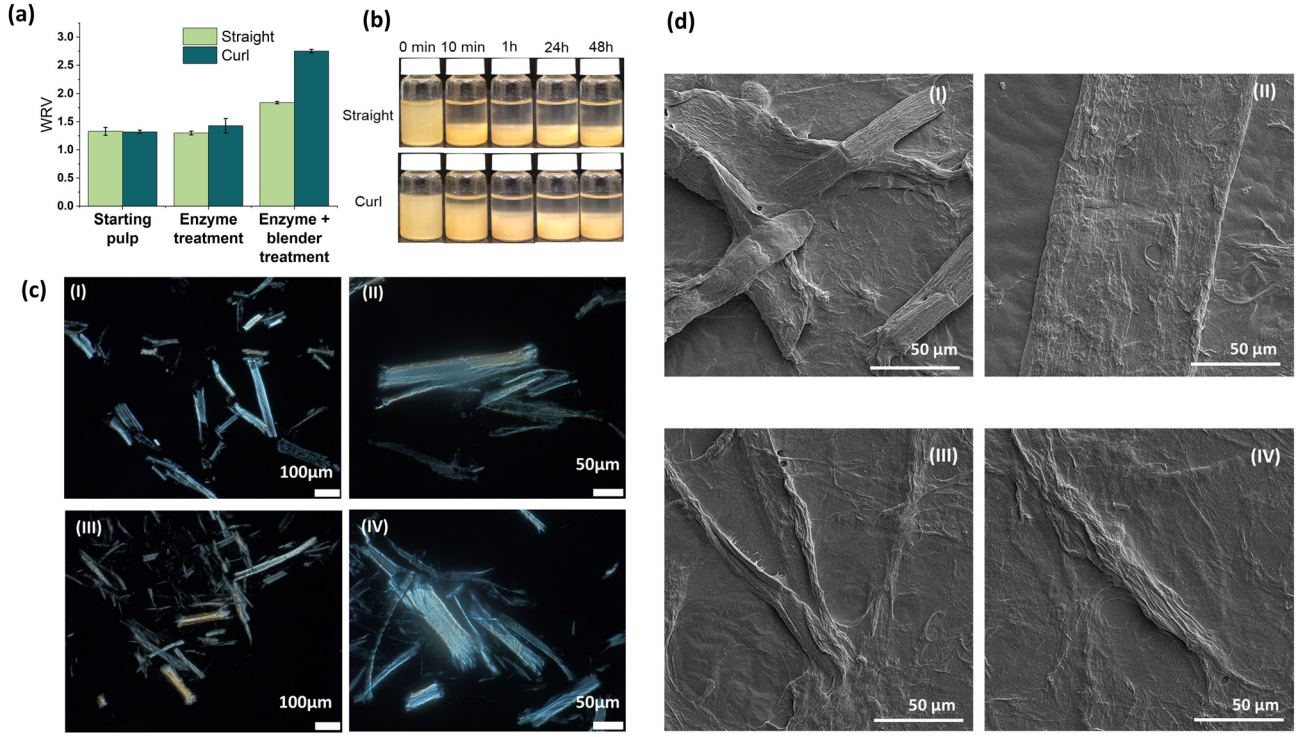

Fig. 3 (a) Water retention value of straight and curl fibers before and after enzyme treatment (mixture lacking CBH activity) and micro-fibrillation (blender) treatment. (b) Settling of micro-fibrillated cellulose suspensions derived from CBH-lacking enzymes treated straight-and-curl fibers. (c) Morphology of straight (I and II) and curl fibers (III and IV) after enzyme treatment and micro-fibrillation under polarized optical microscope. (d) Scanning electron microscope (SEM) images showing the cutting of straight fibers (I and II) and the fibrillation of curl fibers (III and IV) after enzyme treatment and micro-fibrillation.

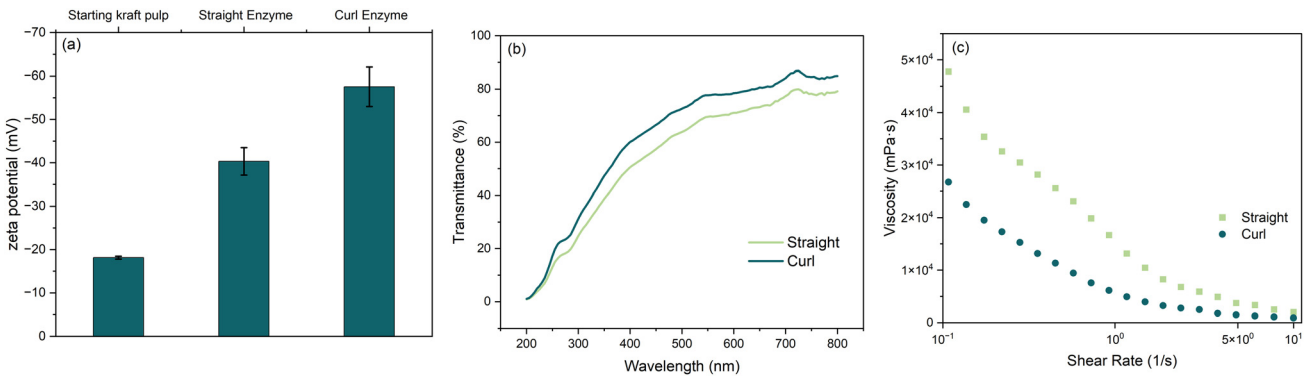

Fig. 4 Zeta-potential (a), transmittance (b) and viscosity (c) of cellulose nano-fibril suspensions made from straight and curl fibers.

fibrillation. Based on the literature, the nano-fibrillation of cellulose is related to several characteristics such as the transmittance and steady-state shear viscosity of the CNF suspensions.[20,40] In this work, it was evident that nanofibrils derived from curl fibers underwent more extensive fibrillation, indicated by their higher suspension (0.05 wt%) transmittance (Fig. 4b) and lower suspension (0.5 wt%) viscosity at all shear rates (Fig. 4c). The higher transmittance of curl-derived CNF provides it with potential application as flexible display substrates, whereas its lower viscosity indicated better dispersion of nanofibrils due to its more organized and less entangled fibril network. It is believed that the greater charge density of curl-derived CNF also contributed to its lower viscosity, as the electrostatic repulsion associated with the surface charge prevented the aggregation/mechanical entanglement of nanofibrils.[40,41] In order to elucidate the morphology of the resulting CNF, transmission electron microscope (TEM) analysis was conducted. By appearance, it was apparent that the

Published on 02 April 2024. Downloaded on 5/26/2026 6:16:00 AM.

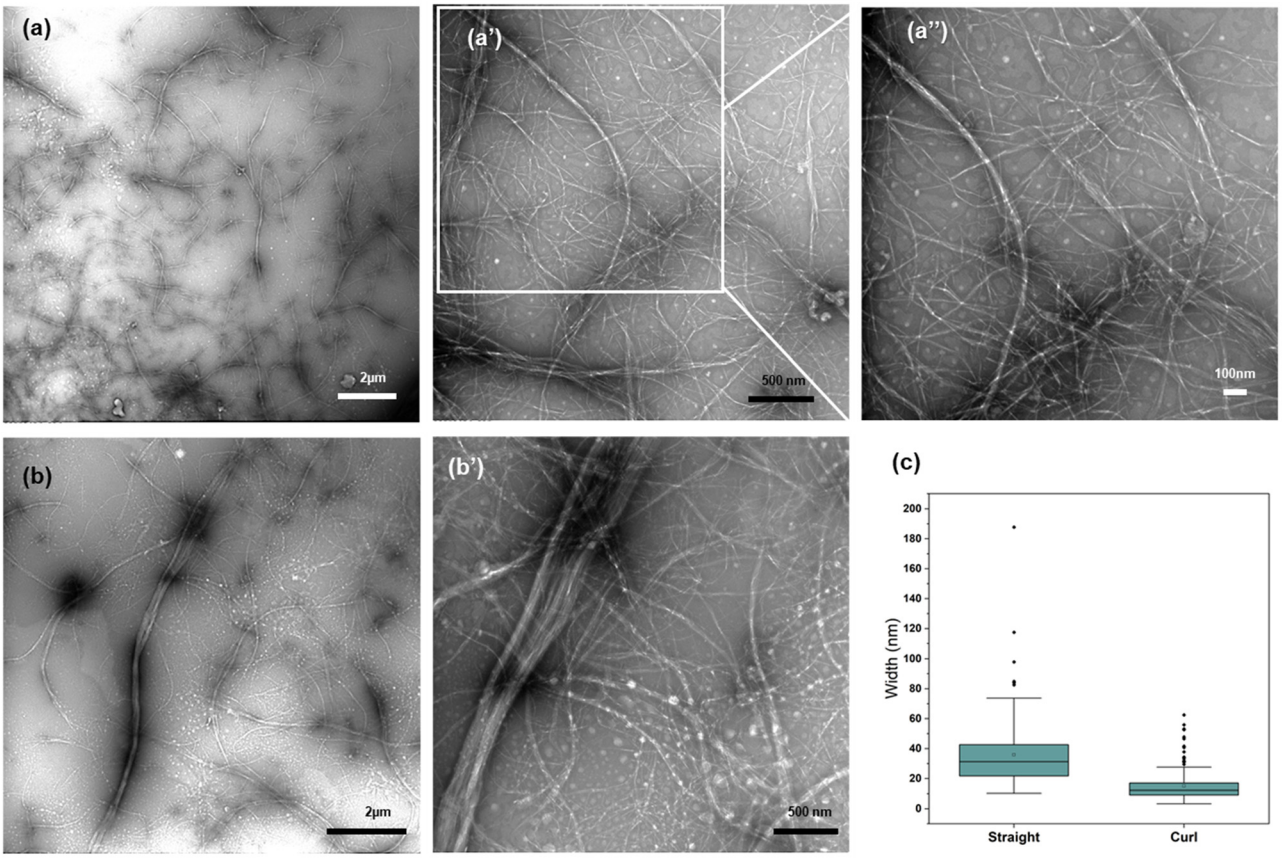

Fig. 5 Morphology (a, a', a'', b and b') and width distribution (c) of cellulose nano-fibrils made from straight (b and b') and curl (a, a' and a'') fibers.

resulting CNF suspensions did contain fibrils at micro level, with some of which being partially separated into nanofibrils (Fig. 5). Overall, curl CNF suspension contained less microfibrils while the nanofibrils were found to be thinner (mostly 5–15 nm) than that of straight CNF suspension (mostly 20–40 nm), indicating a greater degree of nano-fibrillation (Fig. 5). This result shows promise, considering that the average fibril width of CNF obtained through chemical methods like TEMPO oxidation and acid anhydride-mediated esterification typically ranges around 10–20 nm.[42,43]

3.3 Preparation of cellulose nanopaper from nano-fibrillated cellulose

The suspensions of CNF were then transformed into cellulose nanopapers using vacuum filtration, where the nanofibrils were assembled with a random in-plane orientation,[44] followed by air drying, to examine how nano-fibrillation affected the properties of the resulting nanopapers. Both nanopapers demonstrated robust mechanical properties, with tensile strengths exceeding 90 MPa and Young's modulus surpassing 3500 MPa (Fig. 6).

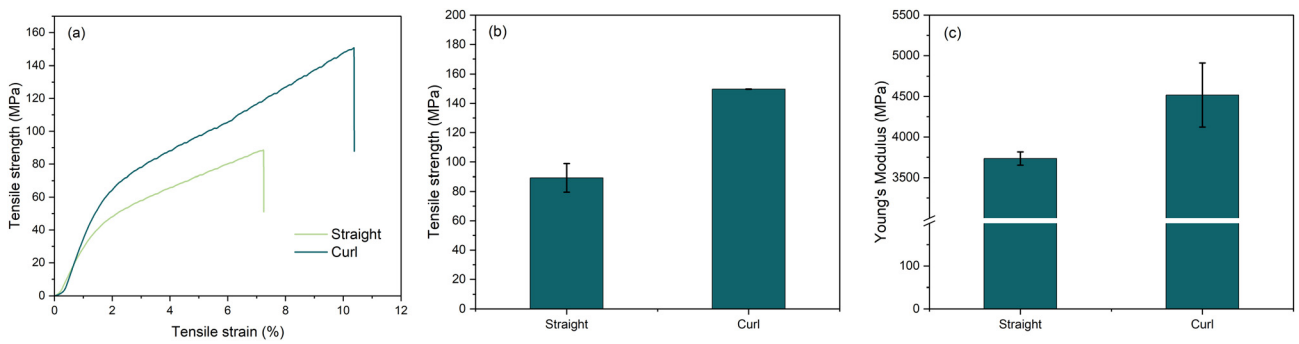

Fig. 6 Tensile stress–strain curves (a), average tensile strength (b) and average Young's modulus (c) of cellulose nanopapers made from cellulose nano-fibrils derived from straight and curl fibers.

 This journal is © The Royal Society of Chemistry 2024

Published on 02 April 2024. Downloaded on 5/26/2026 6:16:00 AM.

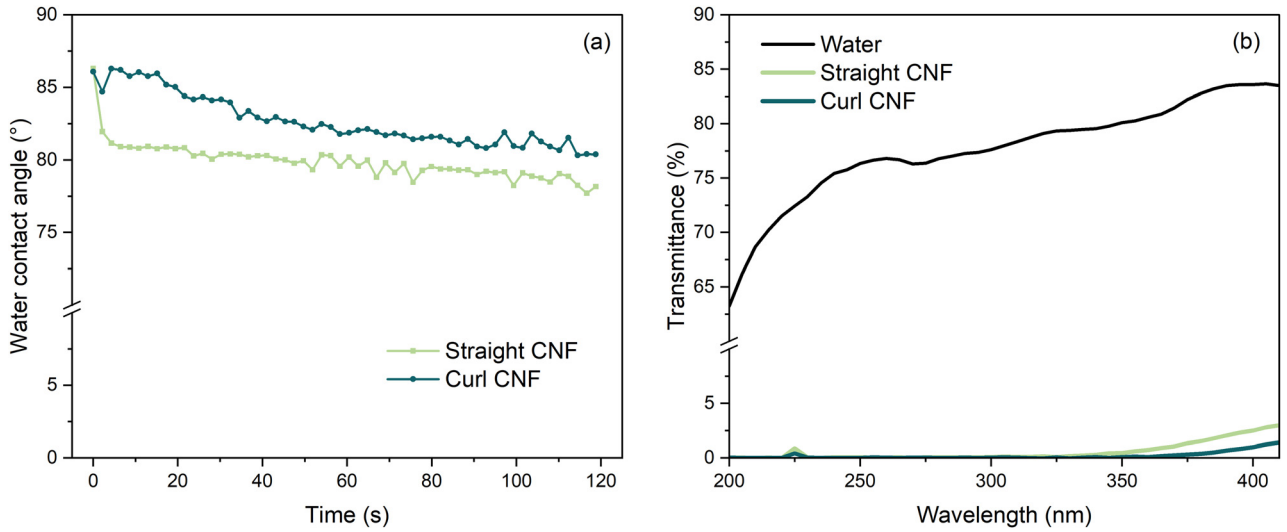

Fig. 7 Water contact angle (a) and transmittance (b) of nanopapers produced from straight and curl fibers-derived cellulose nano-fibrils. In figure b, transmittance of deionized water was reported as "blank".

This result is comparable to CNF derived from chemical pulps through treatments such as acid anhydrides -mediated esterification,[43,45] indicating that the combination of enzymes and mechanical processes was effective as an alternative approach. It is probable that the more organized and less tangled fibril network of curl-derived CNF (due to a higher degree of nano-fibrillation and stronger electrostatic repulsion between nanofibrils) led to a cellulose nanopaper with greater strength compared to the nanopaper derived from straight fibers. As indicated by tensile testing, the cellulose nanopaper derived from the curl-derived CNF exhibited superior characteristics in terms of strain to failure, Young's modulus, and tensile strength compared to the nanopapers produced from straight CNF. Increases of 16%, 17%, and 40% respectively were obtained (Fig. 6).

As mentioned earlier, the use of unbleached softwood kraft pulp in this study provides the opportunity to produce lignin-containing cellulose nanofibrils while minimizing lignin's negative impacts on cellulose-cellulase interaction. The presence of lignin nanoparticles after nano-fibrillation of enzyme-treated pulps was also indicated, as summarized in Fig. 5. To confirm, we next assessed the hydrophobicity of CNF using water contact angle measurement. As the water contact angles of both nanopapers remained at around 80 degrees for 2 minutes (Fig. 7a), this was better than the water contact angle of the CNF derived from untreated cellulose.[46] As well as improved hydrophobicity, another asset of the lignin-containing CNF mixture was its UV-blocking effect. Using the method described by Shao *et al.*,[47] the UV-blocking feature of lignin-containing cellulose nanopapers was also observed, as indicated by low-to-zero transmission rate at wavelength between 200 to 400 nm (Fig. 7b).

4. Conclusions

The introduction of curl-induced disruption of the cellulose fibers significantly enhanced cellulose susceptibility to enzyme treatment, leading to enhanced nano-fibrillation and colloid stability after mechanical treatment. The use of endoglucanase-rich enzyme mixture enhanced the nano-fibrillation of unbleached kraft pulp, resulting in lignin-containing cellulose nanofibrils. These nanofibrils exhibited superior mechanical performance when used to make cellulose nanopapers, indicating that they could be produced with minimum chemical treatments and reduced mechanical refining energy.

Conflicts of interest

The authors declare no conflict of interest.

Acknowledgements

The authors would like to thank Novozymes for generously providing us with the enzymes used in this study and Natural Sciences and Engineering Research Council of Canada (NSERC) for financial support. The authors also thank Mr. Huaiyu Zhang, Mr. Qi Hua, Mr. Dingyuan Zheng, and Mr. Hao Sun for their valuable advice and Mr. Axel Ewashko for his contribution to the initial exploration of this project.

References

1 X. Kang, A. Kirui, M. C. Dickwella Widanage, F. Mentink-Vigier, D. J. Cosgrove and T. Wang, *Nat. Commun.*, 2019, **10**, 1–9.
2 D. J. Cosgrove and M. C. Jarvis, *Front. Plant Sci.*, 2012, **3**, 1–6.
3 Q. Ren, X. Sun, W. Liu, Z. Li, C. Jiang and Q. Hou, *Chem. Eng. J.*, 2023, **456**, 141115.

Published on 02 April 2024. Downloaded on 5/26/2026 6:16:00 AM.

4 T. Yi, H. Zhao, Q. Mo, D. Pan, Y. Liu, L. Huang, H. Xu, B. Hu and H. Song, *Materials (Basel)*, 2020, **13**, 5062.
5 T. Xu, Y. Wang, K. Liu, Q. Zhao, Q. Liang, M. Zhang and C. Si, *Adv. Compos. Hybrid Mater.*, 2023, **6**, 108.
6 H. Liu, T. Xu, C. Cai, K. Liu, W. Liu, M. Zhang, H. Du, C. Si and K. Zhang, *Adv. Funct. Mater.*, 2022, **32**, 2113082.
7 T. Xu, Q. Song, K. Liu, H. Liu, J. Pan, W. Liu, L. Dai, M. Zhang, Y. Wang and C. Si, *Nano-Micro Lett.*, 2023, **15**, 98.
8 W. Liu, Q. Lin, S. Chen, H. Yang, K. Liu, B. Pang, T. Xu and C. Si, *Adv. Compos. Hybrid Mater.*, 2023, **6**, 149.
9 H. Liu, T. Xu, Q. Liang, Q. Zhao, D. Zhao and C. Si, *Adv. Compos. Hybrid Mater.*, 2022, **5**, 1168–1179.
10 G. Albornoz-Palma, D. Ching, S. Henríquez-Gallegos, A. Andrade and M. Pereira, *Cellulose*, 2022, **29**, 8637–8650.
11 R. P. Chandra, J. Wu and J. (John) N. Saddler, *ACS Sustainable Chem. Eng.*, 2019, **7**, 8827–8833.
12 L. G. Thygesen, B. J. Hidayat, K. S. Johansen and C. Felby, *J. Ind. Microbiol. Biotechnol.*, 2011, **38**, 975–983.
13 B. J. Hidayat, C. Felby, K. S. Johansen and L. G. Thygesen, *Cellulose*, 2012, **19**, 1481–1493.
14 A. Khodayari, U. Hirn, S. Spirk, A. W. Van Vuure and D. Seveno, *Cellulose*, 2021, **28**, 6007–6022.
15 D. Dai and M. Fan, *Vib. Spectrosc.*, 2011, **55**, 300–306.
16 V. Arantes, I. K. R. Dias, G. L. Berto, B. Pereira, B. S. Marotti and C. F. O. Nogueira, *Cellulose*, 2020, **27**, 10571–10630.
17 X. Han, R. Bi, V. Khatri, H. Oguzlu, M. Takada, J. Jiang, F. Jiang, J. Bao and J. N. Saddler, *ACS Sustainable Chem. Eng.*, 2021, **9**, 1406–1413.
18 J. Hu, D. Tian, S. Renneckar and J. N. Saddler, *Sci. Rep.*, 2018, **8**, 4–11.
19 G. L. Berto, B. D. Mattos, J. Velasco, B. Zhao, F. Segato, O. J. Rojas and V. Arantes, *Int. J. Biol. Macromol.*, 2023, **243**, 125002.
20 L. Long, D. Tian, J. Hu, F. Wang and J. Saddler, *Bioresour. Technol.*, 2017, **243**, 898–904.
21 S. Koskela, S. Wang, D. Xu, X. Yang, K. Li, L. A. Berglund, L. S. McKee, V. Bulone and Q. Zhou, *Green Chem.*, 2019, **21**, 5924–5933.
22 S. Koskela, L. Zha, S. Wang, M. Yan and Q. Zhou, *Green Chem.*, 2022, **24**, 7137–7147.
23 M. Chemin, K. Kansou, K. Cahier, M. Grellier, S. Grisel, B. Novales, C. Moreau, A. Villares, J. Berrin and B. Cathala, *Biomacromolecules*, 2023, **24**, 3246–3255.
24 I. C. Hoeger, S. S. Nair, A. J. Ragauskas, Y. Deng, O. J. Rojas and J. Y. Zhu, *Cellulose*, 2013, **20**, 807–818.
25 X. Han, R. Bi, H. Oguzlu, M. Takada, J. Jiang, F. Jiang, J. Bao and J. N. Saddler, *ACS Sustainable Chem. Eng.*, 2020, **8**, 14955–14963.
26 K. Liu, H. Du, T. Zheng, W. Liu, M. Zhang, H. Liu, X. Zhang and C. Si, *Green Chem.*, 2021, **23**, 9723–9746.
27 J. Wu, K. Ho, K. Jeong, D. Kim, C. Soo, J. Ha, R. P. Chandra and J. N. Saddler, *Bioresour. Technol.*, 2021, **324**, 124664.
28 J. Wu, R. Chandra and J. Saddler, *Sustainable Energy Fuels*, 2019, **3**, 227–236.
29 J. Jiang, Y. Zhu, S. Zargar, J. Wu, H. Oguzlu, A. Baldelli, Z. Yu, J. Saddler, R. Sun, Q. Tu and F. Jiang, *Ind. Crops Prod.*, 2021, **173**, 114148.
30 J. V. Vermaas, R. Kont, G. T. Beckham, M. F. Crowley, M. Gudmundsson, M. Sandgren, J. Ståhlberg, P. Väljamäe and B. C. Knott, *Proc. Natl. Acad. Sci. U. S. A.*, 2019, **116**, 23061–23067.
31 J. Wu, R. P. Chandra, K. H. Kim, C. S. Kim, Y. Pu, A. J. Ragauskas and J. N. Saddler, *ACS Sustainable Chem. Eng.*, 2020, **8**, 5847–5855.
32 P. Chylenski, B. Bissaro, M. Sørlie, Å. K. Røhr, A. Várnai, S. J. Horn and V. G. H. Eijsink, *ACS Catal.*, 2019, **9**, 4970–4991.
33 M. Eibinger, J. Sattelkow, T. Ganner, H. Plank and B. Nidetzky, *Nat. Commun.*, 2017, **8**, 4–10.
34 L. Brenelli, F. M. Squina, C. Felby and D. Cannella, *Biotechnol. Biofuels*, 2018, **11**, 1–12.
35 T. Ganner, P. Bubner, M. Eibinger, C. Mayrhofers, H. Planks and B. Nidetzky, *J. Biol. Chem.*, 2012, **287**, 43215–43222.
36 L. F. Del Rio, R. P. Chandra and J. N. Saddler, *Bioresour. Technol.*, 2012, **107**, 235–242.
37 S. Tian, J. Jiang, P. Zhu, Z. Yu, H. Oguzlu, A. Balldelli, J. Wu, J. Zhu, X. Sun, J. Saddler and F. Jiang, *ACS Sustainable Chem. Eng.*, 2022, **10**, 10560–10569.
38 F. Gu, W. Wang, Z. Cai, F. Xue, Y. Jin and J. Y. Zhu, *Cellulose*, 2018, **25**, 2861–2871.
39 L. Solhi, V. Guccini, K. Heise, I. Solala, E. Niinivaara, W. Xu, K. Mihhels, M. Kröger, Z. Meng, J. Wohlert, H. Tao, E. D. Cranston and E. Kontturi, *Chem. Rev.*, 2023, **123**, 1925–2015.
40 T. Moberg, K. Sahlin, K. Yao, S. Geng, G. Westman, Q. Zhou, K. Oksman and M. Rigdahl, *Cellulose*, 2017, **24**, 2499–2510.
41 X. Wang, J. Zeng and J. Y. Zhu, *Carbohydr. Polym.*, 2022, **295**, 119885.
42 A. J. Onyianta, M. Dorris and R. L. Williams, *Cellulose*, 2018, **25**, 1047–1064.
43 D. Zheng, X. Sun, H. Sun, Y. Zhu, J. Zhu, P. Zhu, Z. Yu, Y. Ye, Y. Zhang and F. Jiang, *Carbohydr. Polym.*, 2024, **333**, 121961.
44 X. Yang, M. S. Reid, P. Olsén and L. A. Berglund, *ACS Nano*, 2020, **14**, 724–735.
45 M. Beaumont, B. L. Tardy, G. Reyes, T. V. Koso, E. Schaubmayr, P. Jusner, A. W. T. King, R. R. Dagastine, A. Potthast, O. J. Rojas and T. Rosenau, *J. Am. Chem. Soc.*, 2021, **143**, 17040–17046.
46 E. Rojo, M. S. Peresin, W. W. Sampson, I. C. Hoeger, J. Vartiainen, J. Laine and O. J. Rojas, *Green Chem.*, 2015, **17**, 1853–1866.
47 H. Shao, Y. Zhang, H. Pan, Y. Jiang, J. Qi, H. Xiao, S. Zhang, T. Lin, L. Tu and J. Xie, *Int. J. Biol. Macromol.*, 2022, **207**, 917–926.

This journal is © The Royal Society of Chemistry 2024